A Biofilm-Infected Human Clusteroid 3D Co-Culture Platform to Replace Animal Models in Testing Antimicrobial Nanotechnologies

Anhweng Wang,[a] Paul J. Weldrick,[a] Leigh A. Madden [b]and Vesselin N. Paunov[a,c]*

[a] Department of Chemistry and Biochemistry, University of Hull, Cottingham Road, HU67RX, Hull, UK;

[b] Department of Biomedical Sciences, University of Hull, Cottingham Road, Hull, HU67RX, UK;

[c] Department of Chemistry, Nazarbayev University, 53 Kabanbay Batyr Aveue, Nursultan city, 010000, Kazakhstan.

* Corresponding author email: vesselin.paunov@nu.edu.kz

KEYWORDS: clusteroids; 3D culture; biofilm; antibiotic nanocarriers; *P. aeruginosa*; *S. aureus*

ABSTRACT: Microbial biofilms are a major concern in wound care, implant devices and organ infections. Biofilms allow higher tolerance to anti-bacterial drugs, can impair wound healing, and potentially lead to sepsis. There has been a recent focus on developing novel nanocarrier-based delivery vehicles to enhance the biofilm penetration of traditional antibacterial drugs. However, a feasible *in vitro* human skin model to mimic the biofilm formation and its treatment for clearance have not yet been reported. The study describes for the first time the benefits of using an innovative bacterial biofilm-infected keratinocyte clusteroid model. It paves a new way for testing innovative nanomedicine delivery systems in a rapid and reproducible way on a realistic human cell-based platform, free of any animal testing. Herein, we have developed a novel composite 3D biofilm/human keratinocyte clusteroids co-culture platform which was used to measure biofilm clearance efficiency of nanoparticles (NPs)-based therapeutics. We tested this model by treating the biofilm-infected 3D co-culture layers by ciprofloxacin-loaded Carbopol nanogel, surface- functionalized by the cationic protease Alcalase. We measured the antibacterial efficiency of the nanoparticle treatment on clearing *Staphylococcus aureus* and *Pseudomonas aeruginosa* biofilms on the 3D keratinocyte clusteroids/biofilm co-culture model. Our experiments showed that these bacteria can successfully infect the 3D layer of keratinocyte clusteroids and produce a stable biofilm. The biofilms were efficiently cleared by treatment with a formulation of 0.0032 wt % ciprofloxacin-loaded in 0.2 wt % Carbopol NPs surface-functionalized with 0.2 wt % Alcalase. Taken together, these promising results demonstrate that our co-culture model can be exploited as a novel platform for testing the biofilm-eliminating efficiency of various NPs formulations emulating skin and wound infections and could have wider applicability to replace animal models in similar experiments. This 3D cell culture-based platform could help in developing more effective antibacterial agents for clinical applications of antiplaque dental treatments, implants, infection control and wound dressings.

1. INTRODUCTION

Biofilms are a major concern in biomedical, food and environmental fields. The biofilm is a 3D-structured multicellular bacterial colony adhering to the extracellular polymeric substance (EPS) which increases their resistance to various antibiotics.[1] Biofilm formation usually consists of multiple-stages and is associated with expressing of polysaccharides, RNA and DNA.[2] The enhanced structural strength caused by the cell-cell interaction attracts considerable interest on the biofilm formation mechanism.[3] After over 50 years' study since the late seventies when the first definition of biofilms was brought to public attention,[4] most of the human microbiome has been considered to be a complex eco-system of bacterial cells instead of a simple co-existing floating layer. Bacterial biofilms represent a critical component indwelling tissues of various kinds which may become colonized with microorganisms. The first observation of biofilms, aggregated bacteria enclosed within a matrix of extracellular materials, was reported in the lungs of cystic fibrosis (CF) patients.[5,6]

After 50 years of research, biofilms have been detected in the majority of the organs or implanted medical devices within the human body including kidney stones, urinary tract infections, vaginosis and chronic wounds.[7-9] One of the key challenges related to biofilms is chronic wound healing, y caused by pathogens such as *Staphylococcus*, *Klebsiella* and *Pseudomonas* genera.[5,10] The biofilm extra polymer substance (EPS) impairs the wound healing process, as it can potentially inhibit innate inflammatory pathways and resist traditional therapeutics.[11-14] Bacterial invasion of wounds occurs in millions of people every year and increases the burden on managing and treating chronic wounds. The inherent defense and survival mechanisms of microbial biofilms includes avoidance of host inflammatory cells,[5] high tolerance to antibiotics,[15] increase cell-cell interaction making them a remarkably durable feature of the non-healing wound. Until recently, numerous therapeutics have been developed to target biofilms in wounds.

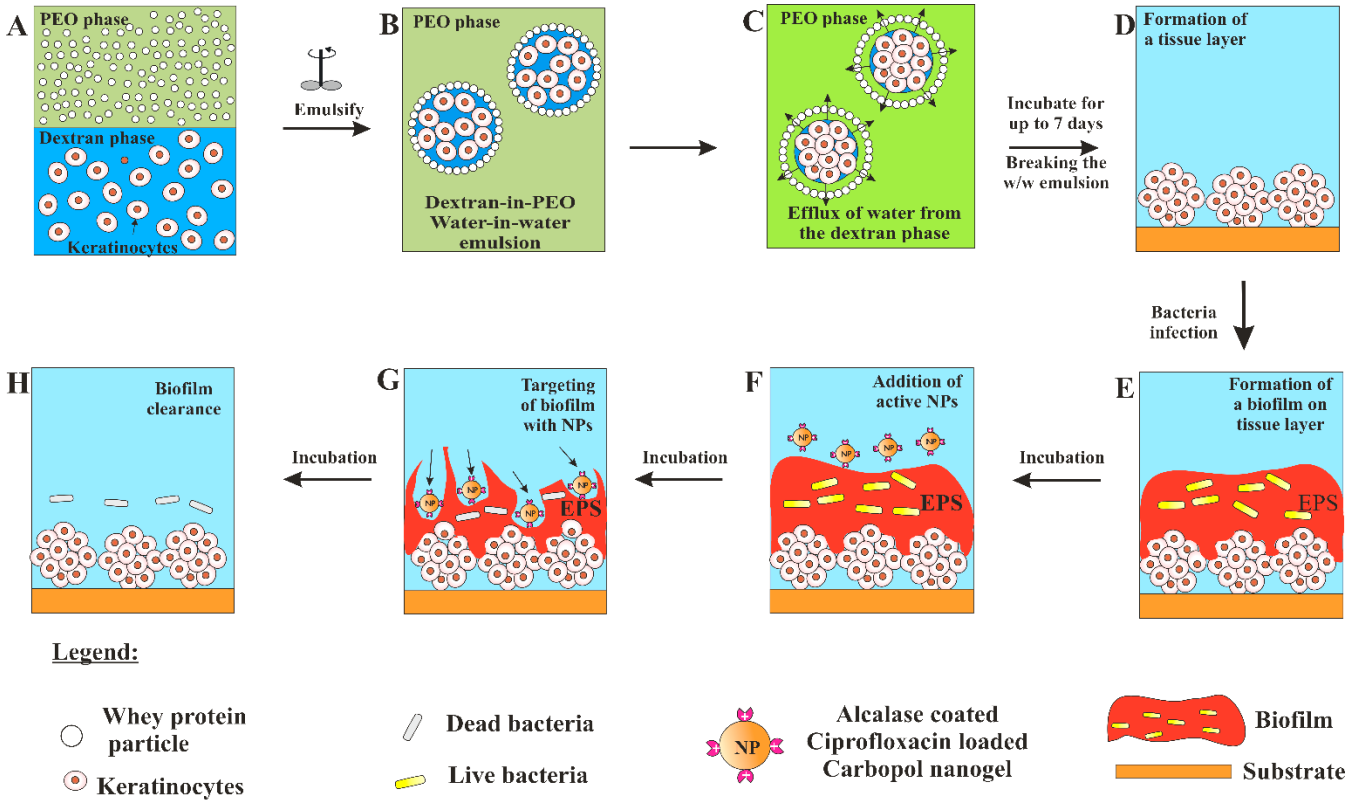

Figure 1. Schematics of the preparation of individual clusteroids and 3D clusteroid layer. (A-D) The HaCaT cells were suspended in the 5.5 wt% DEX in DMEM medium and the suspension was mixed with 5.5 wt% PEO phase by 3 pumps through a syringe. The DEX-in-PEO emulsion drops were then shrunk osmotically by adding a more concentrated PEO solution (11 wt%) to increase the cell-cell contact and facilitate the formation of clusteroids. HaCaT clusteroids were left in the emulsion for 2 h which was then broken down using ten-fold dilution with DMEM medium.[23,30] Clusteroids were then collected and plotted in poly-L-lysine coated 96-well plate to proliferate over 7 days. (E-I) Biofilm formation and clearance of the biofilm utilizing NPs treatment: After the formation of clusteroids layer, 20 µL normalized bacterial suspension culture (*S.aureus* or *P. aeruginosa*) was added to the formed clusteroids layer. Biofilm was formed after overnight incubation at 37ºC with 5% CO_2. 50 µL of 0.0032 wt% ciprofloxacin-loaded 0.2 wt% Alcalase-coated 0.2 wt% Carbopol nanogel particles were used for the biofilm clearance. The cultures were left in incubator for another 12 h before assessing the NPs clearance effect on the biofilm.

The most promising approach is utilizing nanoparticles (NPs) as delivery vehicles to penetrate through the EPS for a deeper clearance of the psoriasis-like biofilm. Antibacterial agents like penicillin, lincomycin, ciprofloxacin and chlorhexidine were generally encapsulated along with metal based nanoparticles (Ag−Au nanocomposite particles, CuONPs, $Mg(OH)_2$NPs, and AuNPs) or silica NPs.[11,16] Weldrick *et al*. have developed an advanced nanomedical formulation based on enzymatic-functionalized NPs which are able to degrade biofilms.[16] The major issues associated with biofilm formation on various tissues or implanted devices urgently require novel in-vivo or in-vivo models in order to avoid using extensive use of

animal models for mimicking this process and exploring various strategies for treatment and biofilm clearance. Such systems can range from simple in-vitro models using microtiter plate assays and agar to flow cells.[17-20] Recent trends in biofilm research have led to numerous studies of in-vitro models for antibacterial susceptibility screening as they are affordable, reproducible and avoid ethical issues associated with in-vivo and animal experiments. However, a considerable amount of literature published on *in vitro* models do not adequately mimic the complexity of the *in-vivo* environment. No previous study has seriously investigated a 3D cell culture platform alternative of in-vivo biofilm testing due to the complex preparation and low yield rate. Recently, we have developed a novel technique for production of tissue clusteroids (cell clusters) from human keratinocytes and hepatocytes (HaCaT and Hep-G2) by trapping them in w/w Pickering emulsion droplets.[21-23] This technique is based on the formation of w/w Pickering emulsions, in which cells are efficiently encapsulated in emulsion droplets, followed by rapid osmotic shrinking of the droplets to compress the cells against each outer and form a large amount of nearly spherical clusteroids in a very short time. The specific aim of this study was to assess the feasibility of utilizing the ATPS based technique to produce clusteroids for generation of an in vitro skin-like tissue. The tissue layer was then co-cultured with bacteria to produce a biofilm which was used as a novel platform for drug testing and delivery test. Here we took this facile method to produce a dense layer of 3D keratinocyte clusteroids in-vitro which was used as the basis for a new platform to form in-vitro biofilm/human cell co-culture and study the effectiveness of specific nanoparticle formulations in in clearing the bacterial biofilm without harming the human 3D Organoids and other *in vitro* platforms provide valuable preclinical screening tools with the ultimate aim of fully replacing animal models.

The present study is the culmination point of three innovative materials science platforms that were developed very recently: (i) A new technique for rapid preparation of large quantities of cells clusteroids which allows rapid formation of model keratinocyte layers.[22,23,30]

(ii) A novel and super-efficient smart antibiotic nanocarrier with a protease surface functionality.[11,16,39]

(iii) Novel nanoparticle-based therapy for targeting antimicrobial resistance,[25]

which were combined here to demonstrate the principle of a new and unique technique for rapid testing the efficiency of nanoparticle formulations on pre-formed bacterial biofilms on human cell layers without doing any animal experiments.

Organoids have potential in this area due to their similarity to their *in vivo* counterpart organs.[31] Most drug candidate failures are attributable to either lack of effectiveness or safety[32] and so there is a need to establish a preclinical model to enable drug testing on primary cells in organoid culture.[33] For example, organoids were produced from both tumor and non-tumor tissue then used in drug testing effectiveness for biliary tract carcinoma.[34] Here, we used HaCaT cells which are widely used as a keratinocyte model due their availability, ease of handling and a phenotype which closely resembles primary keratinocytes.[35,36] HaCaT cells have been shown to be a reliable *in vitro* model to screen drugs in skin diseases and were predicted to become a basis for 3D models to better mimic the skin microenvironment.[37]

We aim to investigate the effectiveness of ciporfloxacin-loaded Carbopol nanogel carriers functionalized with Alcalase 2.4 L FG against a *Staphylococcus aureus*, a Gram-positive bacterium and *Pseudomonas aeruginosa*, a Gram-negative bacterium, both forming a biofilm on the layer of keraticocyte clusteroids. We benchmark the effectiveness of this formulation against

Figure 1illustrates the clusteroids-forming process, its infection with biofilm forming bacteria and subsequent testing of the efficiency of the active nanocarrier to clear up the bacterial biofilm from the 3D cell culture, apparently without adversely impacting the keratinocytes. By surface-functionalizing the nanogel particles with a protease, such as Alcalase 2.4 L FG, the potential of degrading the extracellular polymer substance (EPS) is expected to increase,[16] thus, allowing the ciprofloxacin-loaded Carbopol nanogel carrier to easily access the persistent bacteria “embedded” within the biofilm. Since bacteria have a negatively charged outer cell membrane, the Alcalase-coated ciprofloxacin-loaded Carbopol nanogel particles would electrostatically attach onto their cell walls and release high dose of the loaded antibiotic locally into the bacteria, and ultimately lead to the cells death.[39] The innovation of our model is the demonstration that the novel enzyme-functionalized nanogel carrier of antibiotics can rapidly clear biofilm-forming bacterial infection on a living tissue (clusteroids layer) of human skin cells without affecting the human cell viability.

2. EXPERIMENTAL SECTION

Materials

Carbopol Aqua SF1 nanogel (30 wt% aqueous suspension) was obtained from Lubrizol, USA. The bacteria used in this experiment were purchased from American Type culture collection, as follows, *Staphylococcus aureus subsp. aureus Rosenbach* (ATCC® 29213™) and *Pseudomonas aeruginosa* (Schroeter) Migula (ATCC® 27853™). De-ionized water purified by Milli-Q water system (Millipore) was used in all our studies. Whey protein was bought from No1. Supplements, Suffolk, UK). Sodium alginate, Corning® Transwell® polyester membrane cell culture inserts (96

well plates) and NUNC Cell culture 6-well plates were purchased from Thermo Fisher Scientific (UK). Dextran (MW 500 kDa) and PEO (MW 200 kDa) were purchased from Sigma-Aldrich, UK. Sodium chloride (99.8%) and calcium chloride, Dulbecco's Modified Eagle Medium and Trypsin-EDTA solution were sourced from Fisher Scientific (UK). Mueller-Hilton Broth (MHB), Mueller-Hilton Agar (MHA) were sourced from Oxford, UK. Alcalase 2.4 L FG, EC number; 3.4.21.62 (Novozymes, Denmark) was used to surface-functionalize the Carbopol NPs. Media supplements were fetal bovine serum (10% v/v, Labtech, Heathfield, UK) and 0.25% Trypsin-EDTA (1X, Lonza). MTT colorimetric survival and proliferation kit was sourced from Millipore Corp, USA and used for mammalian cell viability measurement. The poly-L-lysine and alginate lyase was purchased from Sigma Aldrich. All other chemicals were of analytical grade.

2D Keratinocyte Cell Culture

HaCaT cell line culture was purchased from AddexBio (T0020001). The cells were cultured in 10 mL DMEM (Gibco, UK) media supplemented with 10% fetal bovine serum (FBS) and incubated at 37 °C with 5% CO_2 in T75 EasY Flasks (156499) from Thermofisher. The cells were passaged after reaching 70%-80% confluence. Cells were carefully washed with phosphate buffer saline (PBS, Labtech, UK) two times before adding 5 mL 0.25% Trypsin-EDTA (1X, Lonza, UK). The cells were then incubated for 10 min to detach the cells from the flasks. Trypsin-EDTA media was neutralized by adding 10 mL DMEM medium before centrifugation at 400× g for 4 min to isolate the cell pellet. The HaCaT cells were reseeded at a ratio of 1:6 after each passage.

Preparation of the Whey Protein (WP) Particles

The preparation of whey protein (WP) particles was conducted followed by the method similar to the previously reported protocol.[23] Briefly, the whey protein powder was weighted and suspended under agitation for 2h in an aqueous solution at a concentration of 2 wt%. The WP solution was then incubated at 4º C overnight to hydrate the protein. To remove the insoluble residues after the hydration, the solution was centrifugated at 8000×g for 40 min. The supernatant was mixed in a proportion of 1:1 with 0.3 M NaCl solution, followed by dropwise addition of 0.1 M HCl to adjust the pH to 6.18. The heating process was carried out at 82 ºC for 20 min followed by centrifugation at 8000×g to discard the formed sediment. The supernatant was used as WP particle suspension in the following experiments.

Production of cell clusteroid layer

The preparation of clusteroids was slightly modified from the method reported by Celik et al.[23] and Das et al.[30] In summary, PEO aqueous solution (5.5 wt%) was prepared by dissolving an adequate amount of PEO into the heat-treated solution of WP particles to form the continuous phase. A solution of 5.5wt% dextran in DMEM:FBS (9:1) complete medium under sterile conditions was used as a disperse phase (DEX). HaCaT cells were carefully suspended and normalized to adequate cell numbers (1×10^6/mL) in the DEX phase. To encapsulated the HaCaT cells in the emulsion droplets, the DEX phase (with the cells) were transferred to the WP/NaCl /PEO solution and gently homogenized using BD Microlance™3,6, or 12 needles (21G 12, internal diameter 0.512 mm) and a BD Plastipak™ syringe of 1 mL (BD biosciences, Wokingham, UK) by six pumps (in and out). The emulsions were mixed with a PEO solution of higher concentration (14%wt) to a reach a final concentration of 10%wt PEO which is enough to osmotically compress DEX drops and squeeze the entrapped cells into densely packed clusteroids. The emulsions were left in the incubator for two hours to allow the formation of stable cell clusters. The emulsion samples were broken down by adding ten times bigger amount of DMEM complete medium and the clusteroids were collected from the sediment of the suspension after settling under gravity. The viability of clusteroids after at different times in culture was assessed by fluorescence microscopy after treating the cells with fluorescein diacetate (FDA), which is enzymatically converted to fluorescein in the cytoplasm of the viable cells by non-specific esterases. To form 3D clusteroids that would be suitable for the bacterial biofilm/clusteroids co-culture, clusteroids were collected and transferred to a 96 wells culture plate coated with poly-L-lysine instead of alginate gel. The initial cell density of the clusteroids was standardized to 1×10^6 and a 7 days' duration was allowed for the formation of the clusteroids layer.

Bacterial culture and biofilm/clusteroids layers 3D co-culture

Frozen ATCC species (*Staphylococcus aureus* and *Pseudomonas aeruginosa*) were cultured onto MHA plates based on the manufacturer's instruction. The single colony from the MHA Stocks was added into 10 mL of MHB to prepare overnight cultures (O/N cultures). The solution was incubated at 37ºC with 140 rpm shaking. The O/N cultures were diluted into 0.85 wt% sterile saline to achieve the McFarland standard. The optical density of the cultures was adjusted to 0.08-0.12 at 625 nm (FLUO star Omega spectrophotometer, BMP Labtech). A further dilution at ratio of 1:150 into MHB was carried out to the adjusted bacteria suspension to generate working concentrations between 5×10^5 – 1×10^6 colony forming units per mL (CFU mL^{-1}). To visualize the bacteria under fluorescence optical and confocal microscope, Carboxyfluorescein succinimidyl ester (CFSE) was used as a staining dye. CFSE is a fluorescent dye with peak excitation of 494 nm and emission at 521nm that is used to track cells during phagocytosis or monitor cellular division. To achieve the labelling, 1 mL aliquot of the bacterial suspension culture was transferred into a 1.5 mL tube and centrifuged at 4000×g for 5 min to obtain a cell pellet. The supernatant

was discarded, and pellet was resuspended in 2× CFSE working solution. The cells were then incubated at 37ºC with shaking. The CFSE labelled bacteria were collected by centrifugation and the pellet was resuspended in MHB and adjusted between 5×10^5 – 1×10^6 CFU mL^{-1}.

The co-culture of biofilm and clusteroid layer was achieved by adding 20 µL of the either labelled or un-labelled bacterial suspensions to the each well containing the formed clusteroids layer supplemented with 200 µL DMEM complete medium. The bacterial suspension culture was incubated overnight (12 h) at 37ºC to form a biofilm layer on top of the HaCaT 3D culture.

Preparation of ciprofloxacin-loaded nanogel

To date, various methods have been developed and introduced to produce antibacterial NPs. We demonstrate our technique by using a modification of previously reported preparation method for antibiofilm NPs.[16,24,25] Briefly, a 100 mL of 0.2 wt% Carbopol nanogel aqueous suspension was prepared followed by pH adjustment to 7.5 by using 0.25 M NaOH or 0.25M HCl aqueous solution with gentle agitation at 37 °C. 0.0032 wt% ciprofloxacin hydrochloride aqueous solution was obtained by diluting 3.2 mg of the antibiotic (ABX = ciprofloxacin) in 100 mL of deionized water. The pH-adjusted nanogel dispersion was mixed with 100 mL ABX solution and incubated at 37 °C for 30 min to electrostatically bind the cationic antibiotic in the anionic cores of the Carbopol nanogel particles. Another pH adjustment was carried out to reduce the pH of ABX-Carbopol solution to 5.5 by gentle mixing for 30 min. Centrifugation at 6000×g for 30 min was conducted to remove the unencapsulated ABX from the solution and the supernatant was collected for analysis of the encapsulation efficiency. The sediment was collected, carefully rinsed with deionized water and then re-suspended in 100 mL de-ionized water. Again, the pH was adjusted to 7.5 by dropwise addition of 0.25 M NaOH and the solution was left agitating overnight. The pH of the solution was normalized to pH 5.5 using acetate buffer aqueous solution.

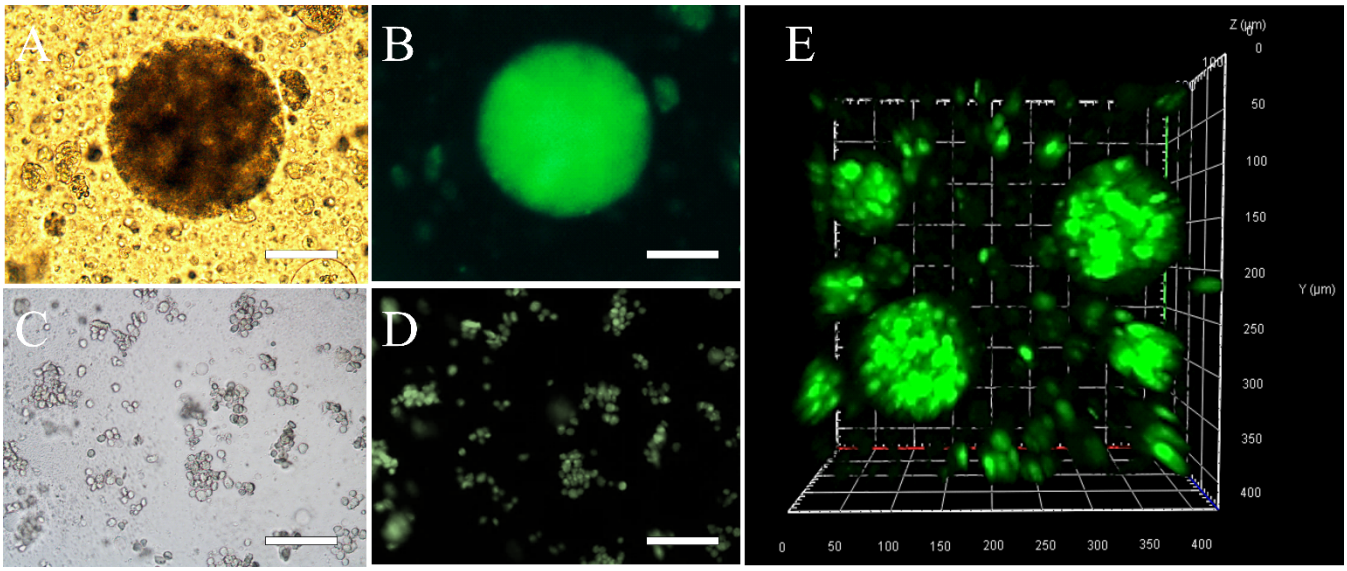

Figure 2. Brightfield images (A, C), fluorescence microscopy images (B, D) and Confocal laser scanning microscope observation (E) of the collected individual clusteroids from the DEX-in-PEO Pickering emulsions. Fluorescein diacetate (FDA) live/dead assay was used to assess the cell viability in the collected clusteroids (B, D, E). The bar is 50 μm for (A, B) and 100 μm for (C, D). The box size is 400 μm×400 μm for (E).

Coating of the ciprofloxacin-loaded Carbopol NPs with Alcalase 2.4 L FG

To obtain a 0.2 wt% solution of Alcalase L FG 2.4, the stock liquid enzyme solution was diluted in de-ionized water to a final volume of 25 mL. Sonication was conducted for 15 min to prevent aggregation. Equal volume (25 mL) of the 0.2 wt% Carbopol Aqua SF1 suspension was mixed with the 0.2 wt% Alcalase FG 2.4 dispersion and pH adjusted to pH 5.5 with gentle agitation for 30 min to electrostatically bind the cationic Alcalase to the anionic surface of the Carbopol NPs. The acquired suspension was then centrifuged at 6000×g for 20 min and the collected pellet was rinsed using deionized water for three times. The pellet was then redispersed into 50 mL deionized water.

To maintain the pH at 5.5, acetate buffer solution was added to the dispersion. Malvern Zetasizer Nano ZS was used to characterize the particle hydrodynamic diameter and zeta potential distributions of the NPs. Before each measurement, 5 min sonication was conducted to the 0.2 wt% Carbopol-0.2 wt% Alcalase dispersion. De-ionized water was used to dilute the dispersion to an appropriate concentration.

Characterization of free Alcalase, Alcalase-nanogel and Alcalase-coated Ciprofloxacin-loaded nanogel

The characterization was performed based on the method introduced by Weldrick et al.[16] To obtain the isoelectric point of the Alcalase L FG 2.4, series of 10 mL of 0.02 wt% Alcalase aqueous solutions were pH-adjusted with 0.25 M HCl or 0.25 M NaOH at a range of pH 5 to 12. Sonication was then performed on each aliquot for 15 min to avoid aggregation. Quartz cuvettes with 1 mL of each aliquot was added to ZEN1002 dip cell to measure the zeta potential. The equipment was set at a refractive index of 1.45 and absorption of 0.001 as per Malvern Instruments protein refractive index manual. All Measurements were conducted at 25°C with three repeats.[11, 16, 25]

Biofilm viability after NP-loaded ciprofloxacin treatment

An O/N bacterial culture was normalized to 1×10^5 CFU/mL in saline and 20 μL aliquot of this culture was plotted to each well in which HaCaT clusteroids layer was grown on. Biofilm was generated after 24 h incubation set at 37°C with 5% CO_2. 0.1 mL of Milli-Q water was considered as the control. 0.2 wt% Carbopol, 0.2 wt% Alcalase 2.4 L FG (diluted in Milli-Q water), and 0.0032 wt% ciprofloxacin-loaded in 0.2 wt% Carbopol nanogel particles coated with 0.2 wt% Alcalase 2.4 L FG were applied as a treatment to measure their biofilm removal ability on the HaCaT clusteroids layer. Similar experiments were also carried out using the individual components of the NPs to prove the efficiency brought by the structure. 0.1 mL of the prepared solution with the same concentration in the NPs were also added into different well plates containing the biofilm/HaCaT clusteroids co-culture models. After 24 h of treatment, the media was discarded and the biofilm/3D clusteroids were carefully collected out of each well. These samples were then put into test tubes which contained 1 mL of new MHB and 2 mL of the sterile glass beads. Each

example was vortexed for 30 secs to disassociate the biofilm and inoculate the MHB with the released residual bacterial cells. The drop plate count technique was utilized to quantify cell CFU/mL. To gauge the viability of bacterial inside the biofilms, we carried out 10-fold dilutions to the MHB. 10 µL solutions were pipetted onto MHA plates and left growing for 24 h at 37ºC. A drop plate enumeration method was employed to calculate the bacterial viability. The last two droplets which contained a countable number of colonies (3 to 30 CFU for every 10 µL drop) were checked and calculated as average for the CFUs.

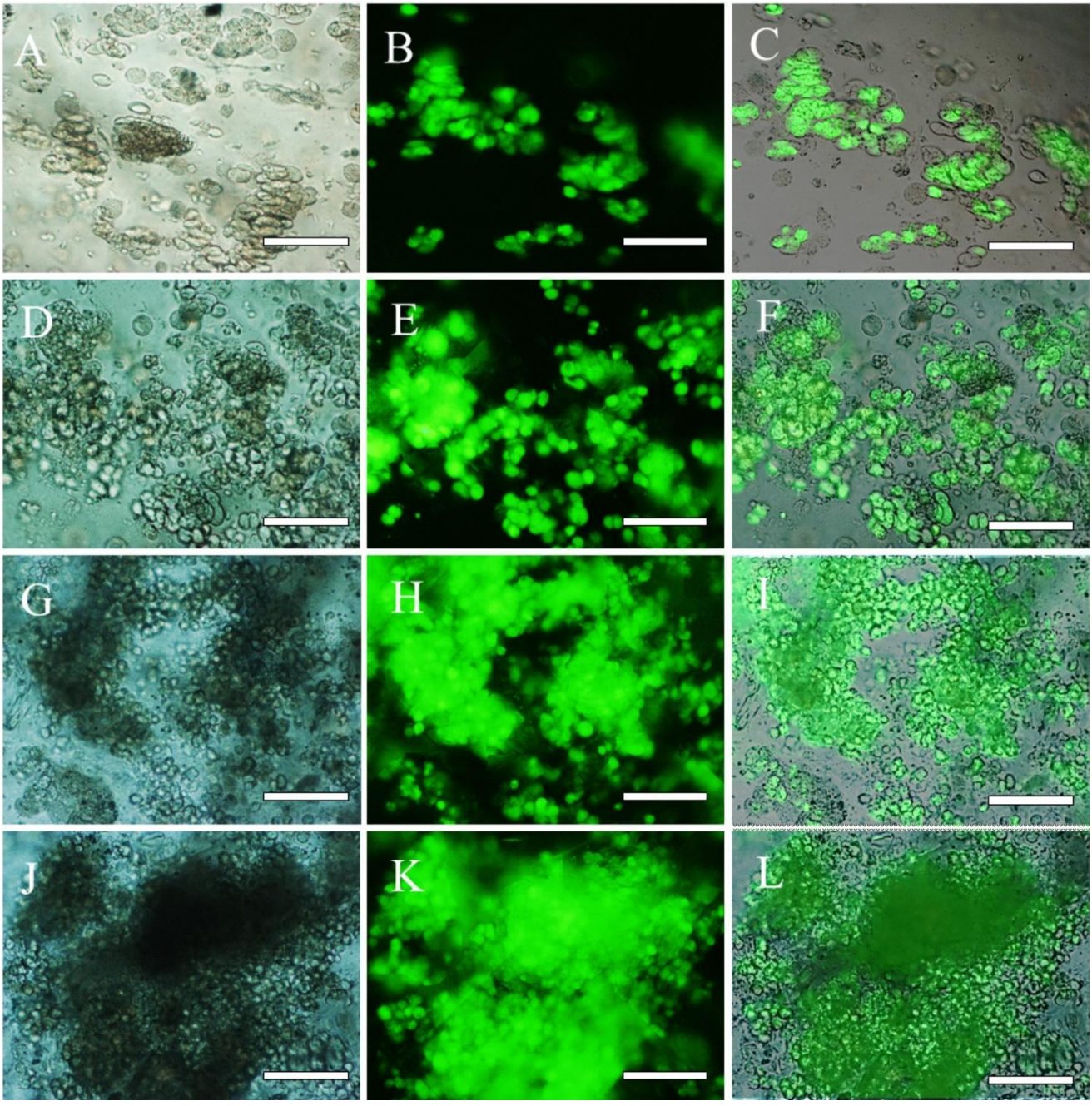

Figure 3. Bright filed microscopy images (A,D,G,J), fluorescence microscopy images (B,E,H,K) and merged (brightfield/fluorescence) images (C,F,I,L) of the clusteroids layer after different days of culture: (A,B,C):Day1: (D,E,F):Day3; (G,H,I):Day5; (J,K,L):Day7. The collected clusteroids were normalized to 1×106 cells per mL equivalent in DMEM medium. 50 µL of the cultures was added to poly-L-lysine coated 96-well plate supplemented with 200 µL DMEM medium. Observations were done by inverted Zeiss DP71 fluorescence microscope at different days of culture. The bar is 100 µm for (A-F) and 200 µm for (G-L).

Optical microscope observation

The microstructure of the clusteroids and the growth pattern of the 3D layered culture of clusteroids were analyzed using an inverted optical microscope (Zeiss Axio Vert.A1 inverted microscope implemented with Olympus IX 71 inverted microscope for field fluorescence microscopy). Samples were observed under various water immersion objectives at ambient temperature (25ºC).

TEM and SEM imaging

The HaCaT clusteroids were gently detached from the well-plate using sterilized loop. The collected clusteroids were carefully adhered to a 7 mm diameter circular glass slide using Carbon discs. The clusteroids were then washed using 10 wt% PBS buffer to remove the excess medium and floating bacterial.

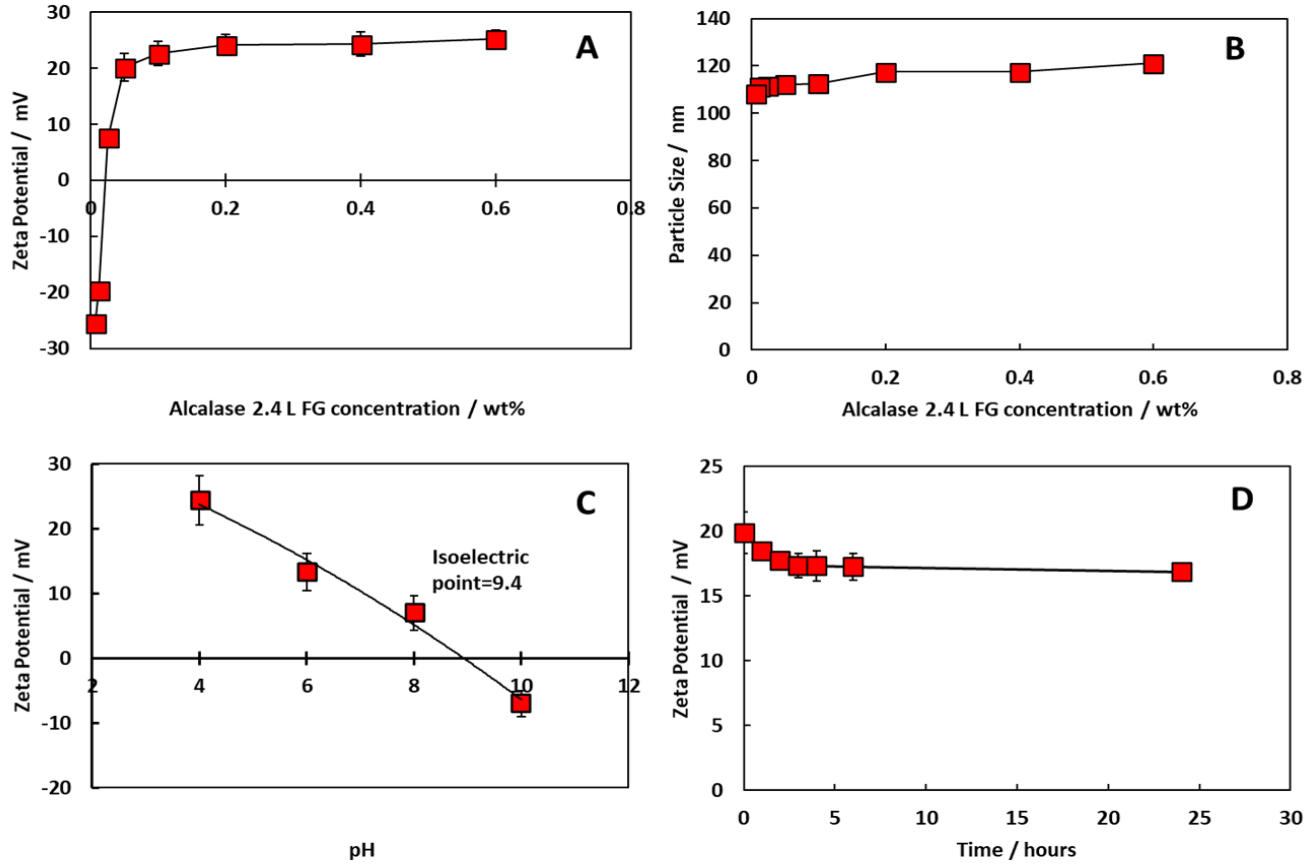

Figure 4. (A) The average zeta-potential of Alcalase 2.4 L FG-coated Carbopol nanogel particles measured at pH 5.5 (acetate buffered saline) with various concentrations of Alcalase mixed with an equal wt% of Carbopol Aqua SF1 NPs. (B) The mean particle hydrodynamic diameter versus the Alcalase 2.4 L FG concentration. (C) Zeta-potential versus pH of the 0.6 wt% Alcalase 2.4 L FG measured using a Malvern Zetasizer Nano ZS at 25 °C. Each value represents a triple replicate with ±S.D. (D) The ζ potential of 0.6 wt % Alcalase 2.4 L FG-coated "empty" 0.6 wt % Carbopol nanogel particles at pH 5.5 (adjusted with acetate buffered saline) measured at various time intervals after preparation.

The cultures were then fixed using 1 wt% glutaraldehyde in PBS buffer at room temperature for 1 h. Glutaraldehyde solution was removed by gentle washing using deionized water. To dehydrate the cultures, the samples were plotted in 0%/75%/90% and absolute ethanol solutions for 30 min, separately. An E3000 Critical Point Dryer (Quorum Technologies, UK) was employed to dry the cultures in the absolute ethanol using CO_2 at its critical point followed by coating with 10 nm carbon film. Imaging of the samples obtained with variable pressure 100 µm aperture at 40 Pa and EHT = 20 kV with probe current 100 pA. Zeiss smart SEM software (Zeiss Evo-60 SEM, Germany) was used to capture the images. One drop of bare Carbopol Aqua NPs, free Alcalase 2.4 L FG protease, and Alcalase-coated Carbopol Aqua SF1 nanogels were

adhered onto coated Copper grids (EM Solutions, UK) with 2 min incubation at room temperature. Excessive substances were removed using deionized water and the samples were negatively stained with 1 wt% aqueous solution of uranyl acetate. The samples were carefully rinsed again using de-ionized water to remove the dye and were left to dry overnight at room temperature. Imaging of the samples were performed using a Jeol 2010 TEM 2010 electron microscope (Jeol, Japan) supplemented with a Gatan Ultrascan 4000 digital camera operating at 120kV.

Confocal laser scanning microscopy (CLSM)

The clusteroids layer was stained using 4′,6-diamidino-2-phenylindole (DAPI) after 7 days of culture. The bacterial cells were pre-stained before the biofilm formation using CFSE to reach long-term tracking, pass through several generations. The visualization of biofilm attached on the clusteroids layer was carried out using CLSM (Zeiss LSM710). The samples were imaged using Z-stacking which is composed of 100 slices for each image with 1 µm per slice. The channels were set to DAPI (461 nm) and FITC (488 nm) for the fluorescence signal of the stained cells and biofilm.

Cytotoxicity assay of the NPs treatment on HaCaT cell clusteroids layer

The influence of the NPs on the viability of the clusteroids layer was carried out using MTT assay. The MTT [3-(4,5-dimethylthiazol-2-yl)-2,5-diphenyltetrazolium bromide] assays were carried out according to the manufacturer's instruction. Briefly,

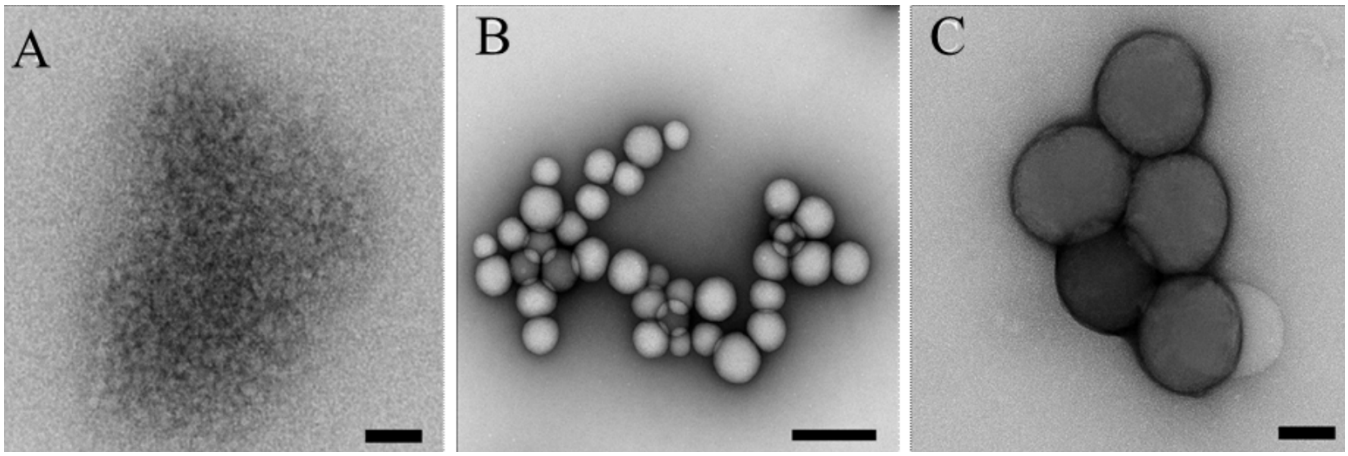

Figure 5. TEM images of (A): Alcalase 2.4 L FG; (B,C): 0.2 wt% Alcalase-coated 0.0032 wt% ciprofloxacin-loaded 0.2 wt% Carbopol NPs. The bars are 50 µm for (A, C) and 100 µm for (B).

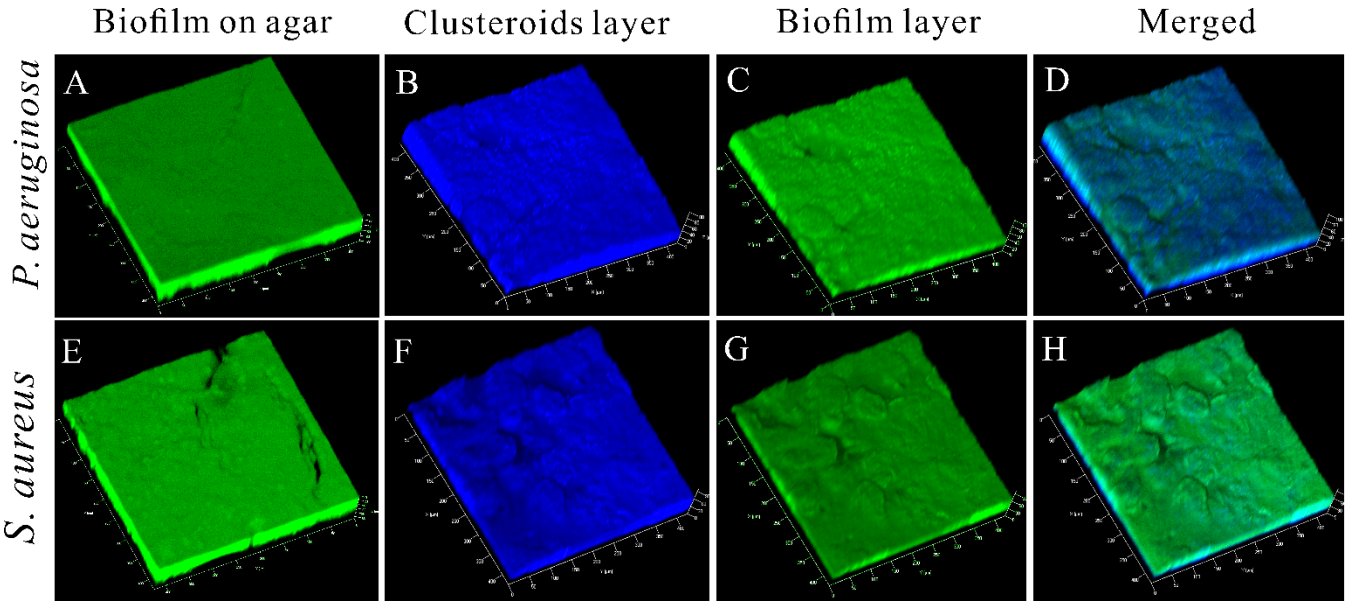

Figure 6. Confocal observation of *S. aureus* (B,D) and *P. aeruginosa* biofilm (F,H) on HaCaT clusteroids layer (B,C,D,F,G,H) or agar (A,E).The observation of the clusteroids layer were stained using DAPI and the biofilms were tracked using CFSE. The x-y axis range is 400 µm × 400 µm.

HaCaT cells clusteroids were treated with 20 µL compound 1, at two separate incubation times (1 h and 24 h). After treatment, the plates were gently shaken and incubated for 4 h at 37°C in 5% CO_2 incubator. The supernatant was removed, 50 µL of isopropanol was added, and the plates were gently shaken to solubilize the formed formazan. The absorbance was measured using a microplate reader at a wavelength of 490 nm. A calibration curve was firstly performed on set amount of HaCaT cells versus absorbance at 490 nm. The viability of the cultures was calculated based on the calibration curved to assess their proliferation.

Cryostat sectioning

As mentioned in the confocal observation section, the clusteroids layer was stained using 4′,6-diamidino-2-phenylindole (DAPI) after the formation of the tissue layer. The bacterial cells were pre-stained before the biofilm formation using CFSE. For these measurements, the clusteroids/biofilm co-cultured samples were firstly fixed in Optimal cutting temperature compound (OCT) and frozen in the freezer overnight. Serial cryostat sections with a thickness of 10 µm through the central region of spheroids were made on Leica CM1950. To visualize the biofilm/clusteroids layer, the sectioned samples were observed using Olympus BX51 fluorescence microscope.

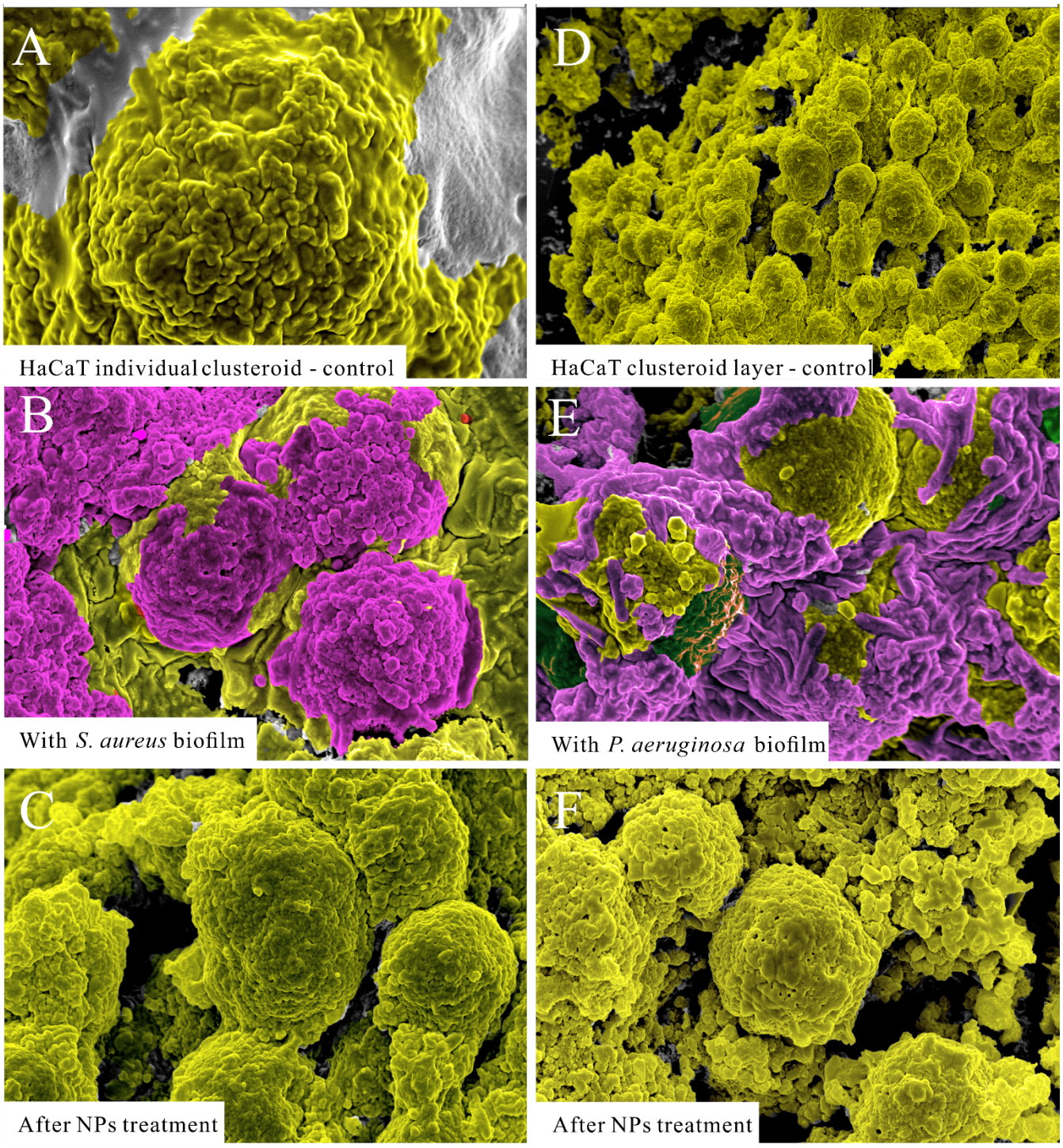

Figure 7. SEM images of: (A) individual un-infected HaCaT cell clusteroids without antibiotic nanocarrier treatment. False color was introduced for aiding the visualization of the bacterial biofilm on the clusteroids layer. The HaCaT cells are colored in yellow and the bacterial biofilms (*S. aureus*, *P. aeruginosa*) are colored in pink. The color was left grey in between the individual clusteroids. (B) *S. aureus* biofilm attached on the 3D culture of HaCaT clusteroid layer; (C) 3D culture of HaCaT clusteroid layer infected with *S. aureus* biofilm after the treatment with Alcalase-coated ciprofloxacin-loaded nanogel particles. (D) 3D culture of un-infected HaCaT clusteroid layer without antibiotic nanocarrier treatment. (E) *P. aeruginosa* biofilm attached on the 3D culture of HaCaT clusteroid layer; (F) HaCaT clusteroid layer infected with *P. aeruginosa* biofilm after the treatment with Alcalase-coated ciprofloxacin-loaded nanogel particles. The bar are 10 μm for (A), 20 μm for (B,C,E,F) and 40 μm for (D). The original SEM images without false color are included in the Supporting Information (Figure S5).

3. RESULTS AND DISCUSSION

Fabrication of HaCaT clusteroids and 3D layers of cell clusteroids

We used the water-in-water Pickering emulsion template to produce the HaCaT cell clusteroids with high yield, prior studies have noted the growth of the clusteroids layer of different cells using W/W Pickering emulsion template including Hep-G2, HEK 293 and HaCaT cells.[21, 23] The clusteroids were collected by breaking down the emulsion system using dilution with DMEM complete medium. As shown in the Figure S1, the clusteroids were successfully obtained from the emulsion droplets with relatively uniform sizes and shapes. The viability of the cells was not affected significantly using this method as shown in the Figure 2.

The collected clusteroids obtained from the emulsion template were placed in a 96-well plate coated with poly-L-lysine to allow the formation of the HaCaT clusteroids layer to mimic the layer of keratinocytes in skin tissue. As shown in the Figure 3, the growth pattern of the HaCaT clusteroids layer was similar to the work done by Celik et al.[23] reported previously. The most obvious observation to emerge from the analysis was that the HaCaT cell clusteroids have grown individually before day 3, and a clear structure of the individual clusteroids could be distinguished. After three days of culture, the clusteroids started to form dense structured tissue. Consistent with other reports in the literature, our research found that clusteroids layer could grow to a relatively integrated skin-liked tissue after seven days of growth which shows excellent potential for an *in vitro* model for biofilm infection. The formed clusteroids layer was used in the following experiments.

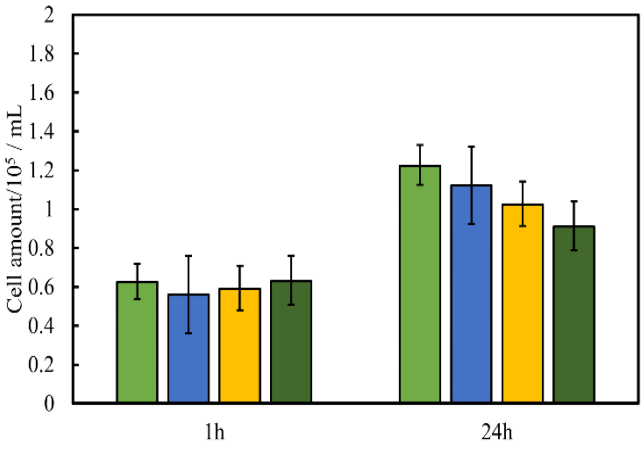

Figure 8. Influence of different concentrations of the Alcalase-coated ciprofloxacin-loaded Carbopol nanogel formulation on the proliferation of the 3D culture of HaCaT clusteroid layer. The cell numbers in the different cultures taken after 1 h and 24 h were normalized by MTT assay. The concentration of the loaded nanogel particles was normalized based on the concentration of the loaded ciprofloxacin. The concentration of the loaded ciprofloxacin is 0 wt% (Control sample-green color), 0.00064 wt%, 0.00107 wt% and 0.00137 wt% (from left to right – blue-yellow-dark green). The cell numbers were normalized by CFU counting.

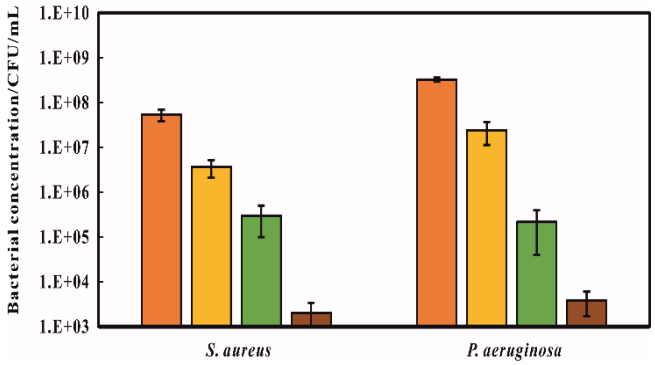

Figure 9. Influence of different concentrations of the Alcalase-coated ciprofloxacin-loaded Carbopol nanogel formulation on the clearance efficiency of *S. aureus* and *P. aeruginosa*
biofilm attached on 3D culture of HaCaT cell clusteroid layer. The concentration of the NPs is normalized based on the concentration of the loaded ciprofloxacin. The concentration of the loaded ciprofloxacin is 0 wt% (Control sample-red colour), 0.00064 wt%, 0.00107 wt% and 0.00137 wt% (from left to right: magenta-yellow-brown color). The cell numbers were normalized by CFU counting.

Encapsulation of ciprofloxacin into Carbopol Aqua SF1 nanogel

We explored the efficiency of using 3D biofilm/keratinocyte clusteroids layer as an alternative *in-vitro* model for drug testing on real human skin or animal models, we designed a nanocarrier delivery system based on enzyme functionalized Carbopol nanogel for biofilm clearance.

Several reports have shown that these nanoparticles exhibited good efficiency in killing the biofilm with low toxicity to the cells. The Carbopol-Alcalase nanoparticle was designed based on the electrical charge at specified a pH value. The lightly cross-linked Carbopol nanogel held a moderate negative charge due to the existence of the carboxylic groups, with zeta-potential of nearly -30 mV at pH 5.5. As shown in the Figure 4C, the Alcalase enzyme was positively charged at pH 5.5, which will facilitate Alcalase immobilization on the Carbopol at this pH due to ionic interactions. The zeta-potential characterization shown in Figure 3A demonstrated that at low Alcalase concentration (below 0.1 wt%), the NPs were negative charged (-20 mV). In contrast, at higher Alcalase concentrated the NPs conferred a positive

charge (+20 mV), which would generate increased killing efficiency of the bacteria in the biofilm.[24, 25] The bare Carbopol nanogel has a size of approximately 110 nm and the Alcalase coating slightly increased the NPs size, with the highest at the concentration of 0.6 wt%, of around 120 nm (Figure 4B). These results confirm that the addition of relatively high concentration of Alcalase turn the NPs cationic without a significant increase in the NPs size. To further examine the stability of the system, the time-corresponded zeta-potential tests were performed. As shown in Figure 4D, the zeta potential readings maintained stable in the range between 16-20 mV over 24 h storage. These results demonstrate that the Alcalase could be deposited electrostatically in the nanogel particles over 24 h, which prove its stability in being used as a carrier system for the enzyme immobilization during treatment.

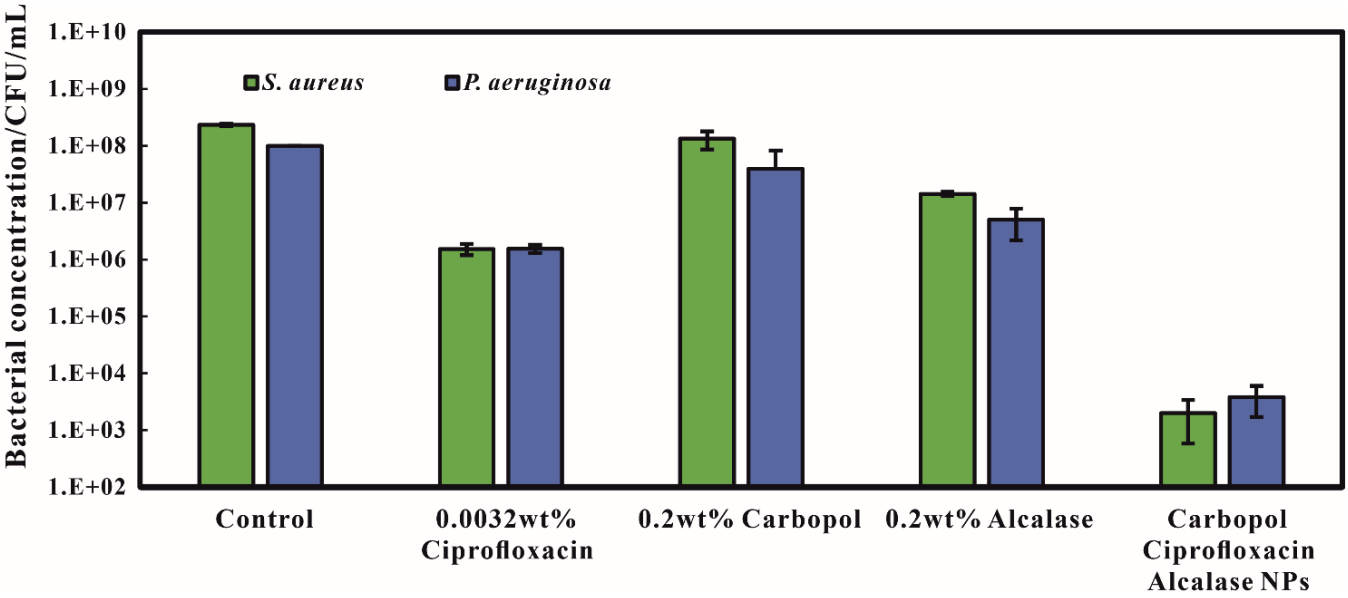

Figure 10. Efficiency of the Alcalase-coated ciprofloxacin-loaded Carbopol nanogel formulation and its individual components on the clearance of *S. aureus* and *P. aeruginosa* biofilms attaching on the 3D culture of HaCaT clusteroids layer. The Alcalase-functionalized ciprofloxacin-loaded Carbopol NPs were compared to equivalent concentrations of the free ciprofloxacin, Carbopol nanogel and Alcalase 2.4 L FG.

Formation of *Staphylococcus aureus* biofilm on the HaCaT clusteroids layer

The first question in this study sought to determine whether we can produce a bacterial biofilm attached on a 3D layer of clusteroids. Several studies have been reported on the biofilm's formation mechanism on agar, various tissues, or implanted devices.[26-28] In this study, the microscopy observation confirmed that *S. aureus* could be successfully anchored on the 3D clusteroids layer (Figure S1). The results shown in the Figures S1 and S2 which used different ways of staining, clearly indicate the formation of the bacterial biofilm on the clusteroids layer. Confocal fluorescence microscopy observation was also carried out to compare the different morphologies of the biofilms formed on agar with these on the clusteroids layer. As could be clearly seen in Figure 4A-D, *S. aureus* had the ability to deposit on both agar plate and a layer of HaCaT cell clusteroids. The biofilm on the agar was shaped completely like a planar bacterial layer while the clusteroids-based bacterial biofilm would shape according to the morphology of the clusteroids. The most obvious finding to emerge from this analysis is that the biofilm also attached on the surface of the layer of living HaCaT cell clusteroids, making this bacterial/3D cell co-culture platform an excellent tool for antibacterial tests. Results obtained from SEM further confirmed the formation of a *S. aureus* biofilm on the cell layer. The Figure 7B confirmed the presence of the sphere-like *S. aureus* bacteria on the clusteroids surface.

Formation of the *Pseudomonas aeruginosa* biofilm on the HaCaT clusteroids layer

S. aureus and *P. aeruginosa* are the most common bacteria isolated from chronic wounds. *S. aureus* is usually detected in the top layer of wounds, while *P. aeruginosa* is localized in the deepest region of wound bed.[29]

Consequently, it would be of great value to understand the mechanisms of *P. aeruginosa* biofilm formation on the clusters of skin cells as this type of cells are likely to be encountered in surface wounds. Similarly, the bright field and fluorescence microscope observation confirmed the existence of the *P. aeruginosa* biofilm on the 3D HaCaT cell clusteroids layer (Figure S3). The confocal

fluorescence microscopy images of the *P. aeruginosa* biofilm on the clusteroids showed a similar structure and appearance of the biofilm compared to the *S. aureus* one (Figure 6). In contrast, one can see the rod-like shape of *P. aeruginosa* in the SEM images of the biofilm coated clusteroids (Figure 7E). These remarkable results suggest that the biofilm/3D cell co-culture could be a promising platform for studying the bacterial biofilm formation on human skin and surface wounds and the clearance efficiency using nanoparticles.

Antibacterial action of the protease-functionalized antibiotic-loaded Carbopol NPs on *Staphylococcus aureus* biofilms

The antibacterial activity of ciprofloxacin-Carbopol NPs on *S. aureus* was examined by incubation of the 3D co-cultured biofilm/clusteroids layer for up to 24 h in solution of different NPs concentrations. Figures 7B and 7C shows SEM images of co-cultured biofilm/clusteroids layer before and after the 24 h treatment with a suspension of 0.0032 wt% ciprofloxacin-loaded 0.2 wt% Carbopol NPs coated with 0.2 wt% Alcalase NPs. The SEM images in Figures 7A and S4B show the morphology of the control sample of untreated individual clusteroids and the 3D layer of clusteroids. These particles would attach on the biofilm/clusteroids 3D layer, which might be attributed to the electrostatic attraction between the cationic protease-functionalized nanogel particle and anionic surface of the biofilm/clusteroids composite.

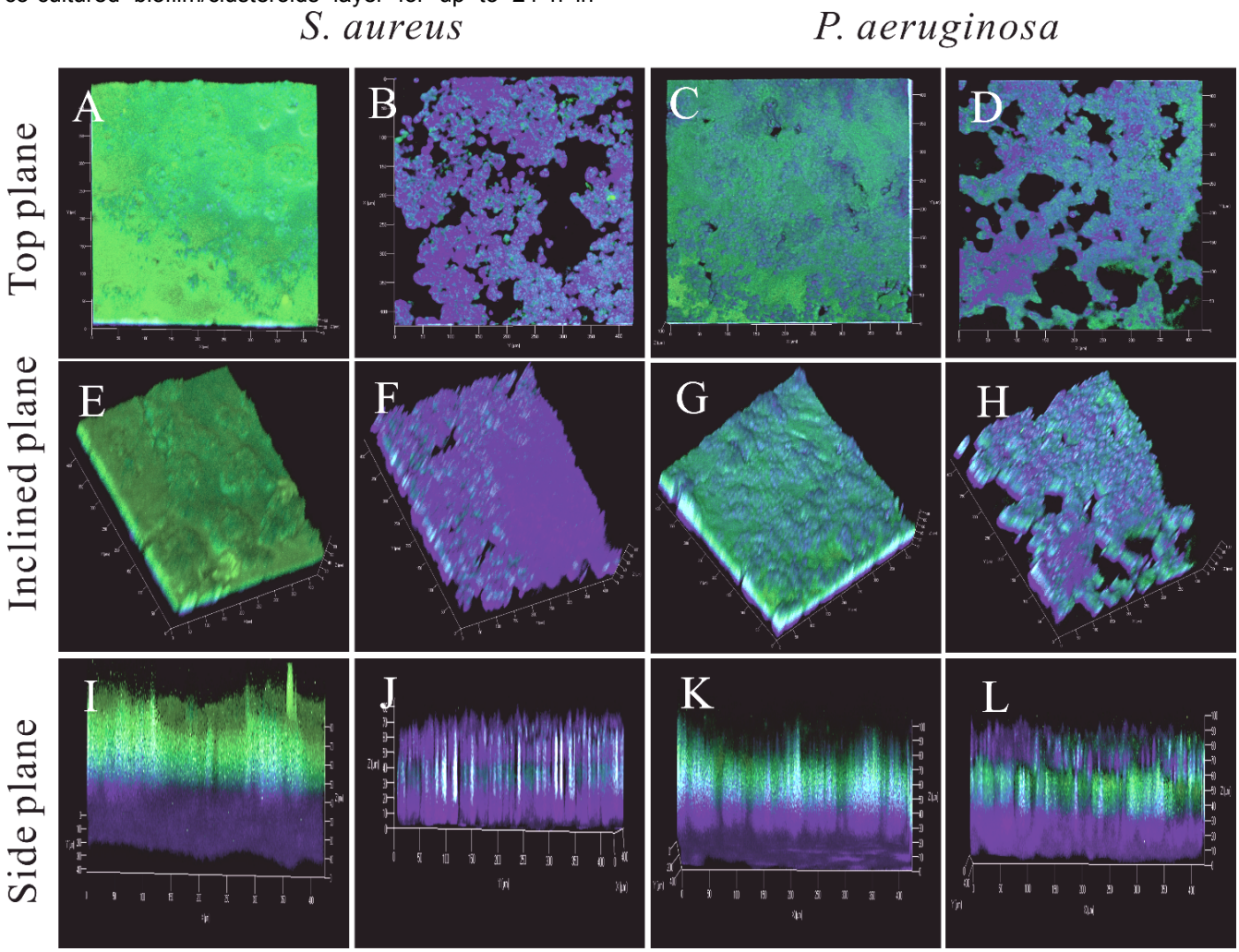

Figure 11. Confocal Z-stacking image of the 3D culture of bacterial biofilm/HaCaT clusteroid layer: (*S. aureus*: A, B, E, F, I, J) and (*P. aeruginosa*: C, D, G, H, K, L). The images show the co-culture before (A, E, I, C, G, K) and after (B, F, J, D, H, L) the treatment with 0.2 wt% Alcalase-coated 0.0032 wt% ciprofloxacin-loaded 0.2 wt% Carbopol NPs. The HaCaT cells were stained using DAPI and the bacteria were pre-stained using CFSE before the formation of the biofilm. The image stacking was done with 100 slices (1 µm per slice). The x-y axis range is 400 µm × 400 µm for (A-H) or 60 µm × 400 µm for (I-L).

As a result, a concentrated protease layer is localized directly on the biofilm surface which facilitates its removal. In addition, the local release of ciprofloxacin from the Carbopol nanocarrier directly onto the bacterial in the clusteroids layers appears to increase their anti-bacterial action.

Figure 9 shows the concentration dependence of the ciprofloxacin-loaded nanocarrier on the *S. aureus* viability. The 3D co-cultured biofilm/clusteroids layers were incubated in a series of NPs suspensions obtained by multiple dilutions of a stock suspension of suspension of 0.0032 wt% ciprofloxacin-loaded 0.2 wt% Carbopol NPs coated with 0.2 wt% Alcalase NPs with DMEM complete medium. This nanocarrier formulation had a clearly stronger antibacterial effect with an increasing concentration of ciprofloxacin. A 5-log decrease of the bacteria CFU/mL was found after 24 h incubation, demonstrating the high anti-bacterial efficiency of these NPs. The SEM images of the clusteroids/biofilm co-culture clearly demonstrate the removal of the biofilm attached on the clusteroids layer and how the original morphology of the 3D clusteroids layer was restored after the treatment. Before the treatment, the clusteroids were nearly completely coated by the biofilm with multiple sphere-like *S. aureus*. The NPs treatment significantly reduced the amount of the visible bacteria anchored on the clusteroids. To investigate the key component in the removal of the biofilm (initially attached on the clusteroids), equivalent concentrations of free Carbopol, free ciprofloxacin as well as the equivalent concentration of free Alcalase (0.2 wt%) were also tested on their capability of biofilm removal on the 3D co-cultured biofilm/clusteroids layer. The bacterial cell viability of all these samples and controls after up to 24 h of incubation were compared with these after treatment of the NPs formulation. One sees that although free ciprofloxacin on its own has significant toxicity against the *S. aureus*, the Carbopol nanocarrier alone (without ciprofloxacin) did not show measurable antibacterial effect when compared with the untreated control sample over the course of the experiment (Figure 10).

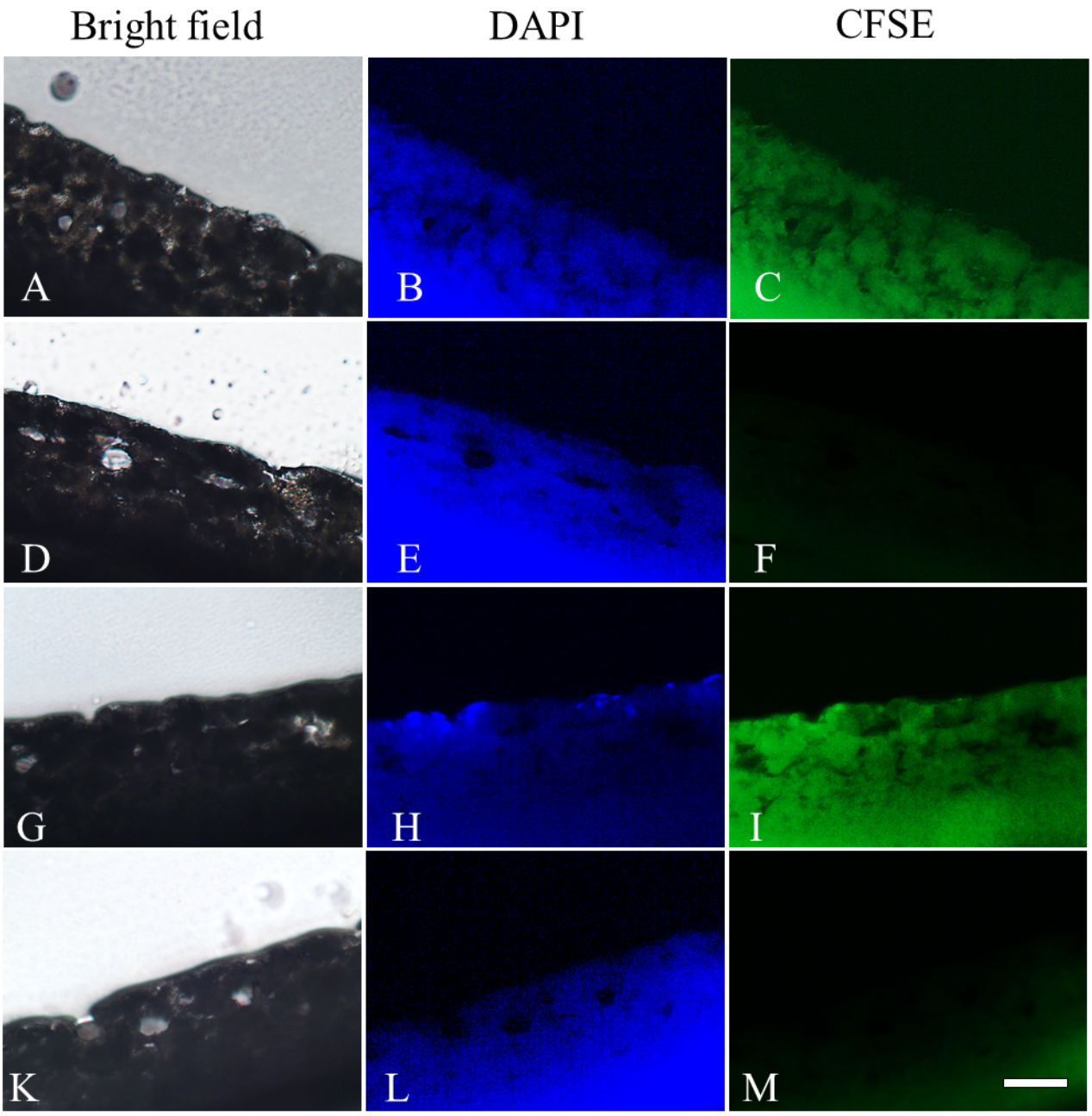

Figure 12. Cryostat sectioning of the 3D co-cultured bacterial biofilm/clusteroids: *S. aureus*(A-F) and *P. aeruginosa*(G-M) biofilm before and after treatment with 0.2 wt% Alcalase-coated 0.0032 wt% ciprofloxacin-loaded 0.2 wt% Carbopol nanogel particles. Each slice obtained from cryo-sectioning is 10 µm. The brightfield and fluorescence microscopy images were taken by using Olympus BX51 fluorescence microscope. The bar is 100 µm (same for all images).

Moreover, the results showed that free Alcalase exhibited similar efficiency in anti-bacterial action compared with an equivalent amount of ciprofloxacin.

According to these data, we can infer that the ciprofloxacin and Alcalase possess the potential to kill the biofilm-forming bacteria (Figure 10). However, 0.0032 wt% ciprofloxacin-loaded 0.2 wt% Alcalase-coated 0.2% Carbopol NPs with the same amount of individual component exhibited 4 orders of magnitude stronger synergistic effect in removing the biofilm, which could be explained by the deep penetration of the enzyme-coated NPS trough the 3D

bacterial biofilm EPS matrix. The electrostatic attraction between the cationic protease-coated ciprofloxacin NPs and the anionic bacterial biofilm would further allow the released ciprofloxacin to disrupt locally the cell membrane causing cell death.

Confocal fluorescence microscopy observation was carried out to provide more detailed information about the biofilm clearance efficiency using the NPs treatment. The CFSE-labeled film decreased significantly after the treatment, its height was reduced from 50 μm to 10 μm (Figure 11). Additionally, we carried out the cryostat sectioning to demonstrate deeper infection of the biofilm. The HaCaT clusteroids were observed as a type of network after the cryostat sectioning (Figure 12). The thickness of the HaCaT clusteroids layer provides itself with the potential to be a platform for biofilm infection and/or biofilm clearance test. As can be seen in Figure 12, the bacterial biofilm nearly covered the whole 3D clusteroids layer before the treatment and was almost completely removed after incubation with antibiotic-loaded NPs with Alcalase-coating.

Anti-bacterial action of protease functionalized Carbopol NPs on *Pseudomonas aeruginosa* biofilms

The antibacterial activity of Alcalase-coated ciprofloxacin-loaded Carbopol NPs on *P. aeruginosa* was also investigated by incubation for up to 24 h at room temperature. Representative SEM images of the control sample of untreated clusteroids layer infected with *P.aeruginosa* are shown in Figure 7E, compared with 3D layers of clusteroid samples treated with the same antibiotic nanocarrier formulation (Figure 7F). One can see that as with the biofilm infection (Figure 7E), the clusteroids have become densely coated with the rod-shaped *P.aeruginosa* before the treatment. After NPs treatment to the 3D clusteroids layer, few bacteria could be observed remaining on the surface of the clusteroids. It should be noted that the threshold of toxicity of the Alcalase-functionalized Carbopol NPs against *P.aeruginosa* is slightly lower than the one for *S.aureus* (Figure 9).

Similarly, Figure 10 compares the viability of *P.aeruginosa* after the NPs treatment as well as with solutions with an equivalent concentration of free Carbopol NPs, free ciprofloxacin, 0.5 wt% Alcalase at the same time in separate experiments. A very similar trend emerges from this comparison, as with the equivalent results with the *S. aureus*. The treatment with the antibiotic-loaded NPs coated with Alcalase shows 4 orders of magnitude higher antibacterial efficiency against *P.aeruginosa* than any other component (Figure 10). Again, the free Alcalase and free ciprofloxacin were benign for the HaCaT clusteroids, and the free Carbopol NPs treatment showed no antimicrobial effect on the *P.aeruginosa* (Figure 10).

Confocal fluorescence microscopy observation and the cryostat sectioning were also carried out to gain more detailed information about the removal of biofilm attached on the surface of 3D clusteroids layer and bacteria penetration in it. Compared to the *S. aureus* biofilm, the infection with *P.aeruginosa* formed a denser and thicker biofilm on the clusteroids layer, achieving an overall thickness of around 70 μm. The clearance effect of the antibiotic-loaded NPs coated with Alcalase on *P.aeruginosa* biofilm was also observed. The cryostat sectioning also showed similar results although weak CFSE-labelled bacterial signals could still be observed. This could be explained by the higher tolerance of *P. aeruginosa* to ciprofloxacin.

4. CONCLUSIONS

We have developed a novel 3D co-cultured biofilm-infected cell clusteroids platform for testing the effect of antibiotic-loaded NPs coated with Alcalase on biofilm clearance effect. We use the previously reported Alcalase-functionalized Carbopol nanocarrier as the testing system. This antibiotic nanocarrier showed a strong enhancement of the antibacterial efficiency compared to the free ciprofloxacin or free Alcalase alone. The toxicity of such NPs to the clusteroids model was insignificant and the clusteroids continue proliferating in the presence of such NPs. We explored the effect of the ciprofloxacin-loaded nanocarrier on the two major bacterial cultures that are associated with biofilm formation in wound care, *S.aureus* and *P.aeruginosa*, respectively.

We demonstrated that this Alcalase-coated ciprofloxacin-loaded nanogel strongly amplifies the antimicrobial action of the antibiotic against both bacterial species after 24 h of incubation. In this experiment, we used confocal, SEM and cryostat sectioning as characterization methods for the detection of biofilm and clusteroids before and after treatment. The Z-stacking image obtained by confocal microscopy clearly demonstrated biofilm formation and subsequent clearance after treatment with NPs formulation. SEM images of the antibiotic nanocarrier-treated clusteroid layers showed the morphology of the biofilm/clusteroids co-culture model before and after the treatment of NPs. Cryostat sectioning was used for detecting the deeper infection of the bacterial and the strong antibacterial effect of the NPs treatment on these biofilm-forming bacteria was also confirmed. The clusteroids/biofilm 3D co-culture model reported here has great potential to be used as an *in vitro* model for wound healing and testing NPs or nanocarrier-based therapeutics for biofilm clearance. This work also demonstrates that this 3D cell biofilm/clusteroids co-culture can give robust results when tested with NPs formulation and has the potential to replace animal models.

In addition, our study clearly demonstrates how ineffective conventional antiseptics and antimicrobials are in targeting formed *S.aureus* biofilms, and how our enzyme-functionalized antibiotic-loaded nanocarriers perform in this context of effectively clearing persistent

biofilms without damaging the infected human cells. Given the tremendous challenge of clearing bacterial biofilms in any environment, we envisage this platform as potentially impactful and significant development in materials science with direct application in the area of biofilm research that can facilitate the development of novel therapies that target antimicrobial resistance.

Supporting information

The supporting information contains: (i) Methods for the biofilm staining with Crystal Violet and Rhodamine; (ii) Microscopy observation and fluorescence observations of the HaCaT clusteroids in the 5.5wt% DEX-in-PEO emulsion droplet; (iii) Microscopy observation of *S.aureus*/Clusteroids layer co-culture mode and *P.aeruginosa* layer co-culture mode different fluorescence filter sets; (iii) Images of Crystal Violet stained *S.aureus* and *P.aeruginosa* biofilm attached on the clusteroids layer; SEM images of the 3D co-culture *S.aureus* biofilm/clusteroids layer models before and after the treatment with 0.0032 wt% ciprofloxacin-loaded 0.2 wt% Alcalase-coated 0.2 wt% Carbopol-NPs; (iv) The original SEM images from Figure 7.

Conflicts of interest

There are no conflicts to declare.

Acknowledgements

A. W. thanks the Chinese Scholarship Council for the financial support of his PhD studies. P.J.W. thanks the University of Hull for the PhD Scholarship.

References

(1) Flemming, H.-C.; Wingender, J. The Biofilm Matrix. *Nat. Rev. Microbiol*. **2010**, *8* (9), 623–633.
(2) Lewis, K. Riddle of Biofilm Resistance. *Antimicrob. Agents Chemother.* **2001**, *45* (4), 999–1007.
(3) Watnick, P.; Kolter, R. Biofilm, City of Microbes. *J. Bacteriol.* **2000**, *182* (10), 2675–2679.
(4) Costerton, J. W.; Geesey, G. G.; Cheng, K.J. How Bacteria Stick. *Sci. Am.* **1978**, *238* (1), 86–95.
(5) Moreau-Marquis, S.; Stanton, B. A.; O'Toole, G.A. Pseudomonas Aeruginosa Biofilm Formation in the Cystic Fibrosis Airway. *Pulm. Pharmacol. Ther*. **2008**, *21* (4), 595–599.
(6) Bjarnsholt, T.; Jensen, P. Ø.; Fiandaca, M. J.; Pedersen, J.; Hansen, C. R.; Andersen, C. B.; Pressler, T.; Givskov, M.; Høiby, N. Pseudomonas Aeruginosabiofilms in the Respiratory Tract of Cystic Fibrosis Patients. *Pediatr. Pulmonol*. **2009**, *44* (6), 547–558.
(7) Kokare, C. R.; Chakraborty, S.; Khopade, A. N.; Mahadik, K. R. Biofilm: Importance and Applications. *Indian J. Biotechnol*. **2009**, *8* (2),159-168
(8) Norsworthy, A. N.; Pearson, M. M. From Catheter to Kidney Stone: The Uropathogenic Lifestyle of Proteus Mirabilis. *Trends Microbiol*. **2017**, *25* (4), 304-315.
(9) Jepson, R. G.; Williams, G.; Craig, J. C. Cranberries for Preventing Urinary Tract Infections. *Cochrane Libr*. **2012**, *10* (10), article no. CD001321.
(10) Davis, S. C.; Ricotti, C.; Cazzaniga, A.; Welsh, E.; Eaglstein, W. H.; Mertz, P. M. Microscopic and Physiologic Evidence for Biofilm-Associated Wound Colonization in Vivo. *Wound Repair Regen*. **2008**, *16* (1), 23-29.
(11) Weldrick, P. J.; Hardman, M. J.; Paunov, V. N. Smart Active Antibiotic Nanocarriers with Protease Surface Functionality Can Overcome Biofilms of Resistant Bacteria. *Mater. Chem. Front*. **2021**, 5 (2), 961−972.
(12) Scotland, K. B.; Lo, J.; Grgic, T.; Lange, D. Ureteral Stent-Associated Infection and Sepsis: Pathogenesis and Prevention: A Review. *Biofouling* **2019**, *35* (1), 117–127.
(13) Minasyan, H. Sepsis: Mechanisms of Bacterial Injury to the Patient. Scand. *J. Trauma Resusc. Emerg. Med*. **2019**, 27 (1), article no. 19.
(14) Klingenberg, C.; Aarag, E.; R??nnestad, A.; Sollid, J. E.; Abrahamsen, T. G.; Kjeldsen, G.; Flaegstad, T. Coagulase-Negative Staphylococcal Sepsis in Neonates: Association between Antibiotic Resistance, Biofilm Formation and the Host Inflammatory Response. *Pediatr. Infect. Dis. J*. **2005**, *24* (9), 817–822.
(15) Høiby, N.; Bjarnsholt, T.; Givskov, M.; Molin, S.; Ciofu, O. Antibiotic Resistance of Bacterial Biofilms. *Int. J. Antimicrob. Agents* **2010**, *35* (4), 322–332.
(16) Weldrick, P. J.; Hardman, M. J.; Paunov, V. N., Enhanced Clearing of Wound-Related Pathogenic Bacterial Biofilms Using Protease-Functionalized Antibiotic Nanocarriers. *ACS Appl. Mater. Interf.* **2019**, *11* (47), 43902-43919.
(17) Gilbertie, J. M.; Schnabel, L. V.; Hickok, N. J.; Jacob, M. E.; Conlon, B. P.; Shapiro, I. M.; Parvizi, J.; Schaer, T. P. Equine or Porcine Synovial Fluid as a Novel Ex Vivo Model for the Study of Bacterial Free-Floating Biofilms That Form in Human Joint Infections. *PLoS One* **2019**, *14* (8), article no. e0221012.
(18) Salli, K. M.; Ouwehand, A. C. The Use of in Vitro Model Systems to Study Dental Biofilms Associated with Caries: A Short Review. *J. Oral Microbiol*. **2015**, *7* (1), 26149.
(19) Gurjala, A. N.; Geringer, M. R.; Seth, A. K.; Hong, S. J.; Smeltzer, M. S.; Galiano, R. D.; Leung, K. P.; Mustoe, T. A. Development of a Novel, Highly Quantitative in Vivo Model for the Study of Biofilm-Impaired Cutaneous Wound Healing: Animal Model for Biofilm-Impaired Wound Healing. *Wound Repair Regen*. **2011**, *19* (3), 400–410.
(20) Coenye, T.; Nelis, H. J. In Vitro and in Vivo Model Systems to Study Microbial Biofilm Formation. *J. Microbiol. Methods* **2010**, *83* (2), 89–105.
(21) Wang, A.; Madden, L. A.; Paunov, V. N. High-Throughput Fabrication of Hepatic Cell Clusteroids with Enhanced Growth and Functionality for Tissue Engineering Applications. *Mater. Adv*. **2020**, *1* (8), 3022–3032.
(22) Wang, A.; Madden, L. A.; Paunov, V. N. Advanced Biomedical Applications Based on Emerging 3D Cell Culturing Platforms. J. Mater. Chem. B Mater. Biol. Med. 2020, 8 (46), 10487–10501.
(23) Celik, S. B. G.; Dominici, S. R.; Filby, B. W.; Das, A. A. K.; Madden, L. A.; Paunov, V. N. Fabrication of Human Keratinocyte Cell Clusters for Skin Graft Applications by Templating Water-in-Water Pickering Emulsions. *Biomimetics (Basel)* **2019**, *4* (3), 50.
(24) Halbus, A. F.; Horozov, T. S.; Paunov, V. N. Strongly Enhanced Antibacterial Action of Copper Oxide Nanoparticles with Boronic Acid Surface Functionality. *ACS Appl. Mater. Interfaces* **2019**, *11* (13), 12232–12243.
(25) Weldrick, P. J.; Iveson, S.; Hardman, M. J.; Paunov, V. N. Breathing New Life into Old Antibiotics: Overcoming

Antibacterial Resistance by Antibiotic-Loaded Nanogel Carriers with Cationic Surface Functionality. *Nanoscale* **2019**, *11* (21), 10472–10485.
(26) Dusane, D. H.; Lochab, V.; Jones, T.; Peters, C. W.; Sindeldecker, D.; Das, A.; Roy, S.; Sen, C. K.; Subramaniam, V. V.; Wozniak, D. J.; Prakash, S.; Stoodley, P. Electroceutical Treatment of Pseudomonas Aeruginosa Biofilms. *Sci. Rep*. **2019**, *9* (1), 2008.
(27) Arciola, C. R.; Campoccia, D.; Montanaro, L. Implant Infections: Adhesion,Biofilm Formation and Immune Evasion. *Nat. Rev. Microbiol*. **2018**, *16* (7), 397–409.
(28) Ammann, T. W.; Bostanci, N.; Belibasakis, G. N.; Thurnheer, T. Validation of a Quantitative Real-Time PCR Assay and Comparison with Fluorescence Microscopy and Selective Agar Plate Counting for Species-Specific Quantification of an in Vitro Subgingival Biofilm Model. *J. Periodontal Res*. **2013**, *48* (4), 517–526.
(29) Gilbertie, J. M.; Schnabel, L. V.; Hickok, N. J.; Jacob, M. E.; Conlon, B. P.; Shapiro, I. M.; Parvizi, J.; Schaer, T. P. Equine or Porcine Synovial Fluid as a Novel Ex Vivo Model for the Study of Bacterial Free-Floating Biofilms That Form in Human Joint Infections. *PLoS One* **2019**, *14* (8), article no. e0221012.
(30) Das, A.A.K.; Filby, B.W.; Geddes, D.A.; Legrande, D.; Paunov, V.N. High Throughput Fabrication of Cell Spheroids by Templating Water-in-Water Pickering emulsions, *Mater. Horiz*., **2017**, *4* (6), 1196−1200.
(31) Takahashi, T. Organoids for Drug Discovery and Personalized Medicine. *Annu. Rev. Pharmacol. Toxicol.* **2019**, *59* (1), 447–462.
(32) Vaidya, V. S.; Ferguson, M. A.; Bonventre, J. V. Biomarkers of Acute Kidney Injury. *Annu. Rev. Pharmacol. Toxicol.* **2008**, *48* (1), 463–493.
(33) Harrison, R. K. Phase II and Phase III Failures: 2013-2015. *Nat. Rev. Drug Discov.* **2016**, *15* (12), 817–818.
(34) Driehuis, E.; Kretzschmar, K.; Clevers, H. Establishment of Patient-Derived Cancer Organoids for Drug-Screening Applications. *Nat. Protoc.* **2020**, *15* (10), 3380–3409.
(35) Deyrieux, A. F.; Wilson, V. G. In Vitro Culture Conditions to Study Keratinocyte Differentiation Using the HaCaT Cell Line. *Cytotechnology* **2007**, *54* (2), 77–83.
(36) Sprenger, A.; Weber, S.; Zarai, M.; Engelke, R.; Nascimento, J. M.; Gretzmeier, C.; Hilpert, M.; Boerries, M.; Has, C.; Busch, H.; Bruckner-Tuderman, L.; Dengjel, J. Consistency of the Proteome in Primary Human Keratinocytes with Respect to Gender, Age, and Skin Localization. *Mol. Cell. Proteomics* **2013**, *12* (9), 2509–2521.
(37) Colombo, I.; Sangiovanni, E.; Maggio, R.; Mattozzi, C.; Zava, S.; Corbett, Y.; Fumagalli, M.; Carlino, C.; Corsetto, P. A.; Scaccabarozzi, D.; Calvieri, S.; Gismondi, A.; Taramelli, D.; Dell'Agli, M. HaCaT Cells as a Reliable in Vitro Differentiation Model to Dissect the Inflammatory/Repair Response of Human Keratinocytes. Mediators Inflamm. 2017, 2017, article no. 7435621.
(38) Weldrick, P. J.; Hardman, M. J.; Paunov, V. N. Superenhanced Removal of Fungal Biofilms by Protease‐Functionalized Amphotericin B Nanocarriers. Adv NanoBio Res 2021, 1 (2), article no. 2000027.
(39) Weldrick, P.J., San, S., Paunov, V.N., Advanced Alcalase-Coated Clindamycin-Loaded Carbopol Nanogels for Removal of Persistent Bacterial Biofilms, ACS Appl. Nano Mater. 2021, 4, 1187–1201.

Table of Contents artwork

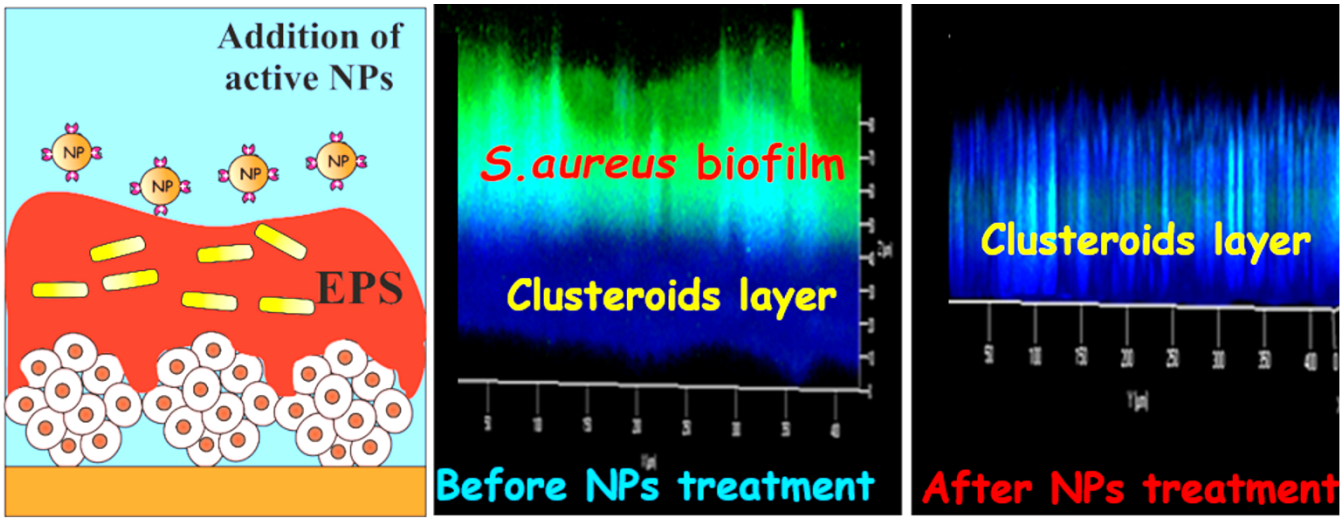
Addition of active NPs
NP
NP
NP
NP
EPS
S.aureus biofilm
Clusteroids layer
Before NPs treatment
Clusteroids layer
After NPs treatment